

A peer-reviewed version of this preprint was published in PeerJ on 4 July 2019.

[View the peer-reviewed version](https://peerj.com/articles/7265) (peerj.com/articles/7265), which is the preferred citable publication unless you specifically need to cite this preprint.

Trubl G, Roux S, Solonenko N, Li Y, Bolduc B, Rodríguez-Ramos J, Eloefadrosch EA, Rich VI, Sullivan MB. 2019. Towards optimized viral metagenomes for double-stranded and single-stranded DNA viruses from challenging soils. PeerJ 7:e7265 <https://doi.org/10.7717/peerj.7265>

Towards optimized viral metagenomes for double-stranded and single-stranded DNA viruses from challenging soils

Gareth Trubl^{1,2}, Simon Roux³, Natalie Solonenko¹, Yueh-Fen Li¹, Benjamin Bolduc¹, Josué Rodríguez-Ramos^{1,4}, Emiley A. Eloie-Fadrosch³, Virginia I. Rich^{Corresp., 1}, Matthew B. Sullivan^{Corresp., 1, 5}

¹ Department of Microbiology, Ohio State University, Columbus, Ohio, United States

² Physical and Life Sciences Directorate, Lawrence Livermore National Laboratory, Livermore, California, United States

³ Joint Genome Institute, Department of Energy, Walnut Creek, California, United States

⁴ Department of Soil and Crop Sciences, Colorado State University, Fort Collins, Colorado, United States

⁵ Civil, Environmental and Geodetic Engineering, Ohio State University, Columbus, Ohio, United States

Corresponding Authors: Virginia I. Rich, Matthew B. Sullivan

Email address: virginia.isabel.rich@gmail.com, mbsulli@gmail.com

Soils impact global carbon cycling and their resident microbes are critical to their biogeochemical processing and ecosystem outputs. Based on studies in marine systems, viruses infecting soil microbes likely modulate host activities via mortality, horizontal gene transfer, and metabolic control. However, their roles remain largely unexplored due to technical challenges with separating, isolating, and extracting DNA from viruses in soils. Some of these challenges have been overcome by using whole genome amplification methods and while these have allowed insights into the identities of soil viruses and their genomes, their inherent biases have prevented meaningful ecological interpretations. Here we experimentally optimized steps for generating quantitatively-amplified viral metagenomes to better capture both ssDNA and dsDNA viruses across three distinct soil habitats along a permafrost thaw gradient. First, we assessed differing DNA extraction methods (PowerSoil, Wizard mini columns, and cetyl trimethylammonium bromide) for quantity and quality of viral DNA. This established PowerSoil as best for yield and quality of DNA from our samples, though ~1/3 of the viral populations captured by each extraction kit were unique, suggesting appreciable differential biases among DNA extraction kits. Second, we evaluated the impact of purifying viral particles after resuspension (by cesium chloride gradients; CsCl) and of viral lysis method (heat vs bead-beating) on the resultant viromes. DNA yields after CsCl particle-purification were largely non-detectable, while unpurified samples yielded 1-2-fold more DNA after lysis by heat than by bead-beating. Virome quality was assessed by the number and size of metagenome-assembled viral contigs, which showed no increase after CsCl-purification, but did from heat lysis relative to bead-beating. We also evaluated sample preparation protocols for ssDNA virus recovery. In both CsCl-purified and non-purified samples, ssDNA viruses were successfully

recovered by using the Accel-NGS 1S Plus Library Kit. While ssDNA viruses were identified in all three soil types, none were identified in the samples that used bead-beating, suggesting this lysis method may impact recovery. Further, 13 ssDNA vOTUs were identified compared to 582 dsDNA vOTUs, and the ssDNA vOTUs only accounted for ~4% of the assembled reads, implying dsDNA viruses were dominant in these samples. This optimized approach was combined with the previously published viral resuspension protocol into a sample-to-virome protocol for soils now available at protocols.io, where community feedback creates 'living' protocols. This collective approach will be particularly valuable given the high physicochemical variability of soils, which will may require considerable soil type-specific optimization. This optimized protocol provides a starting place for developing quantitatively-amplified viromic datasets and will help enable viral ecogenomic studies on organic-rich soils.

1 Introduction

2 Optimization of experimental methods to generate viral-particle metagenomes
3 (viromes) from aquatic samples has enabled robust ecological analyses of marine viral
4 communities (reviewed in Brum and Sullivan 2015; Sullivan, Weitz, and Wilhelm 2016; Hayes et
5 al. 2017). In parallel, optimization of informatics methods to identify and characterize viral
6 sequences has advanced viral sequence recovery from microbial-cell metagenomes, as well as
7 virome analyses (Edwards and Rohwer 2005; Wommack et al. 2012; Roux et al. 2015; Brum &
8 Sullivan, 2015; Roux et al. 2016; Bolduc et al. 2016; Ren et al. 2017; Amgarten et al. 2018).
9 Application of these methods with large-scale sampling (Brum et al. 2015; Roux et al. 2016) has
10 revealed viruses as important members of ocean ecosystems acting through host mortality,
11 gene transfer, and direct manipulation of key microbial metabolisms including photosynthesis
12 and central carbon metabolism during infection, via expression of viral-encoded 'auxiliary
13 metabolic genes' (AMGs). More recently, the abundance of several key viral populations was
14 identified as the best predictor of global carbon (C) flux from the surface oceans to the deep
15 sea (Guidi et al. 2016). This finding suggests that viruses may play a role beyond the viral shunt
16 and help form aggregates that may store C long-term. These discoveries in the oceans have
17 caused a paradigm shift in how we view viruses: no longer simply disease agents, it is now clear
18 that viruses play central roles in ocean ecosystems and help regulate global nutrient cycling.

19 In soils, however, viral roles are not so clear. Soils contain more C than all the vegetation
20 and the atmosphere combined (between 1500–2400 gigatons; Lehmann and Kleber 2015), and
21 soil viruses likely also impact C cycling, as their marine counterparts do. However, our
22 knowledge about soil viruses remains limited due to the dual challenges of separating viruses
23 from the highly heterogeneous soil matrix, while minimizing DNA amplification inhibitors (e.g.
24 humics; reviewed in Williamson et al. 2017). For these reasons, most soil viral work is limited to
25 direct counts and morphological analyses (i.e. microscopy observations), from which we have
26 learned (i) there are 107–109 viruses/g soil, (ii) viral morphotype richness is generally higher in
27 soils than in aquatic ecosystems, and (iii) viral abundance correlates with soil moisture, organic
28 matter content, pH, and microbial abundance (reviewed in Williamson 2017; Narr et al. 2017).
29 Thus, while sequencing data for soil viruses are hard to come by, such high particle counts and
30 patterns suggest that viruses also play important ecosystems roles in soils.

31 The first barrier to obtaining sequence data for soil viruses is simply separating the viral
32 particles from the soil matrix, and then accessing their nucleic acids. Viral resuspension is
33 unlikely to be universally solvable with a single approach due to high variability of soil
34 properties (e.g. mineral content and cation exchange capacity) impacting virus-soil interactions.
35 There have been independent efforts to optimize virus resuspension methods tailored to
36 specific soil types, and employing a range of resuspension methods (reviewed in Narr et al.
37 2017; Pratama and van Elsas, 2018). Once viruses are separated, extraction of their DNA must
38 surmount the additional challenges of co-extracted inhibitors (hampering subsequent
39 molecular biology, as previously described for soil microbes; Narayan et al. 2016; Zielińska et al.
40 2017), and low DNA yields.

41 While little empirical data are available for inhibitors in soil viral extractions, there have
42 been a diversity of approaches to compensate for low DNA yields. Two widely used methods
43 are multiple displacement amplification (MDA; ‘whole genome’ amplification using the phi29
44 polymerase) and random priming-mediated sequence-independent single-primer amplification
45 (RP-SISPA). Both allow qualitative observations of viral sequences, but preclude quantitative
46 ecological inferences. Specifically, MDA causes dramatic shifts in relative abundances of DNA
47 templates, which impact subsequent estimates of viral populations diversity, and, most
48 dramatically, over-amplify ssDNA viruses (Binga, Lasken, and Neufeld, 2008; Yilmaz, Allgaier,
49 and Hugenholtz 2010; Kim, Whon, and Bae 2013; Marine et al. 2014). RP-SISPA is biased
50 towards the most abundant viruses or largest genomes, and leads to uneven coverage along
51 the amplified genomes (Karlsson, Belák, and Granberg 2013). More recently, quantitative
52 amplification methods have emerged that use transposon-mediated tagmentation (Nextera, for
53 dsDNA; Trubl et al. 2018; Segobola et al. 2018) or acoustic shearing to fragment and a custom
54 adaptase (Accel-NGS 1S Plus, for dsDNA and ssDNA; Roux et al. 2016; Rosario et al. 2018) to
55 ligate adapters to DNA templates, before PCR amplification is used to obtain enough material
56 for sequencing. These approaches have successfully amplified as little as 1 picogram (Nextera
57 XT; Rinke et al. 2016) and 100 nanograms (Accel-NGS 1S Plus; Kurihara et al. 2014) of input DNA
58 for viromes while maintaining the relative abundances of templates.

59 We previously optimized a viral resuspension method for three soil habitats (palsa, bog,
60 and fen, spanning a permafrost thaw gradient; Trubl et al. 2016). Given emerging quantitative,
61 low-input DNA library construction options, we sought here to characterize how the choice of
62 methods for viral particle purification, lysis and DNA extraction impacted viral DNA yield and
63 quality, and resulting virome diversity. We tested three different DNA extraction methods, and
64 then two virion lysis methods with and without further particle purification. The extracted DNA
65 was prepared for sequencing using the Accel-NGS 1S Plus kit, generating quantitative soil
66 viromes including both ssDNA and dsDNA viruses, enabling a robust comparison of the different
67 protocols tested.

68 **Methods**

69 *Field site and sampling*

70 Stordalen Mire (68.35°N, 19.05°E) is a peat plateau in Arctic Sweden in a zone of
71 discontinuous permafrost. Peat depth ranges from 1–3 meters (Johansson et al. 2006; Normand
72 et al. 2017). Habitats broadly span three stages of permafrost thaw: palsa (drained soil,
73 dominated by small shrubs, and underlain by intact permafrost), bog (partially inundated peat,
74 dominated by Sphagnum moss, and underlain by partially thawed permafrost), and fen (fully
75 inundated peat, dominated by sedges, and with no detectable permafrost at <1 m) (further
76 described in Hodgkins et al. 2014). These soils vary chemically (Hodgkins et al., 2014; Normand
77 et al. 2017; Wilson et al. 2017), hydraulically (Christensen et al. 2004; Malmer et al. 2005;
78 Olefeldt et al. 2012; Jonasson et al. 2012), and biologically (Mondav et al. 2014; McCalley et al.
79 2014; Mondav et al. 2017; Woodcroft et al. 2018), creating three distinct habitats. Soil was

80 collected with an 11 cm-diameter custom circular push corer at palsa sites, and with a 10 cm ×
81 10 cm square Wardenaar corer (Eijkelkamp, The Netherlands) at the bog and fen sites. Three
82 cores from each habitat were processed using clean techniques described previously (Trubl et
83 al. 2016) and cut in five-centimeter increments from 1–40 cm for palsa and 1–80 cm for bog
84 and fen cores. Samples were flash-frozen in liquid nitrogen and kept at –80°C until processing.
85 The sampled palsa, bog, and fen habitats were directly adjacent, such that all cores were
86 collected within a 120 m radius. For this work, viruses were analyzed from 20–24 cm deep
87 peat, from three cores at each of the three habitats. For Experiment 1 (DNA extraction), 18
88 samples were used (9 bog and 9 fen), with 10 ± 1 g of soil per sample. For Experiment 2 (virion
89 lysis and purification), 36 samples were used (12 palsa, 12 bog, and 12 fen) with 7.5 ± 1 g of soil
90 per sample.

91 *Experiment 1: Optimizing DNA extraction*

92 Viruses were resuspended using a previously optimized method for these soils (Trubl et
93 al. 2016) with minor adjustments. Briefly, 10 ml of a 1% potassium citrate resuspension buffer
94 amended with 10% phosphate buffered-saline, 5 mM ethylenediaminetetraacetic acid, and 150
95 mM magnesium sulfate was added to 10 ± 0.5 g peat. Viruses were physically dispersed via 1
96 min of vortexing, 30 s of manual shaking, and then 15 min of shaking at 400 rpm at 4 °C. The
97 samples were then centrifuged for 20 min at $1,500 \times g$ at 4 °C to pellet debris, and the
98 supernatant was transferred to new tubes. The resuspension steps above were repeated two
99 more times and the supernatants were combined, and then filtered through a 0.2 µm
100 polyethersulfone membrane filter to remove particles and cells and transferred into a new 50
101 ml tube. The filtrate was then purified via overnight treatment with DNase I (ThermoFisher,
102 Waltham, Massachusetts) at a 1:10 dilution at 4°C, inactivated by adding a final concentration
103 of 10 mM EDTA and EGTA and mixing for 1 hour. All viral particles were further purified by CsCl
104 density gradients, established with five CsCl density layers of ρ 1.2, 1.3, 1.4, 1.5, and 1.65
105 g/cm³; we included a 1.3 g/cm³ CsCl layer to collect ssDNA viruses (Thurber et al. 2009). After
106 density gradient centrifugation of the viral particles, we collected and pooled the 1.3–1.52
107 g/cm³ range from the gradient for viral DNA extraction. The viral DNA was extracted (same
108 elution volume) using one of three methods: Wizard mini columns (Wizard; Promega, Madison,
109 WI, products A7181 and A7211), cetyl trimethylammonium bromide (CTAB; Porebski, Bailey,
110 and Baum 1997), or DNeasy PowerSoil DNA extraction kit with heat lysis (10 min incubation at
111 70°C, vortexing for 5 s, and 5 min more of incubation at 70°C) (PowerSoil; Qiagen, Hilden,
112 Germany, product 12888). The extracted DNA was further cleaned up with AMPure beads
113 (Beckman Coulter, Brea, CA, product A63881). DNA purity was assessed with a Nanodrop 8000
114 spectrophotometer (Implen GmbH, Germany) by the reading of A260/A280 and A260/A230,
115 and quantified using a Qubit 3.0 fluorometer (Invitrogen, Waltham, Massachusetts). DNA
116 sequencing libraries were prepared using Swift Accel-NGS 1S Plus DNA Library Kit (Swift
117 BioSciences, Washtenaw County, Michigan), and libraries were determined to be ‘successful’ if
118 there was a smooth peak on the Bioanalyzer with average fragment size of <1kb (200–800 bp
119 ideal) and minimal-to-no secondary peak at ~200 bp (representing concatenated adapters) (Fig.

120 S1), and <20 PCR cycles were required for sequencing. Six libraries were successful (two from
121 bog and four from fen) and required 15 PCR cycles. The successful libraries were sequenced
122 using Illumina HiSeq (300 million reads, 2 x 100 bp paired-end) at JP Sulzberger Columbia
123 Genome Center.

124 *Experiment 2: Optimizing particle lysis and purification*

125 Viromes were generated as in Experiment 1 with minor changes. First, viruses were
126 resuspended as described for Experiment 1, except half of the samples were not purified with
127 CsCl density gradient centrifugation. Second, DNA was extracted from all samples using the
128 PowerSoil method, but the physical method of particle lysis was tested by half of the samples
129 undergoing the standard heat lysis as above and the other half undergoing the alternative
130 PowerSoil bead-beating step (with 0.7 mm garnet beads). Third, the extracted DNA was further
131 cleaned up with DNeasy PowerClean Pro Cleanup Kit (Qiagen, Hilden, Germany, product
132 12997), instead of AMPure beads. Assessment of microbial contamination was done via qPCR
133 (pre and post-cleanup) with primer sets 1406f (5'-GYACWCACCGCCCGT-3') and 1525r (5'-
134 AAGGAGGTGWTCARCC-3') on 5 µl of sample input to amplify bacterial and archaeal 16S rRNA
135 genes as previously described (Woodcroft et al. 2018). Finally, the 12 palsa samples were
136 sequenced at the Joint Genome Institute (JGI; Walnut creek, CA), where library preparation was
137 performed using the Accel-NGS 1S Plus kit. All viromes required 20 PCR cycles, except -CsCl,
138 bead-beating which required 18. All libraries were sequenced using the Illumina HiSeq-2000
139 1TB platform (2 x 151 bp paired-end).

140 *Bioinformatics and statistics*

141 The same informatics and statistics approaches were applied to viromes from
142 Experiments 1 and 2. The sequences were quality-controlled using Trimmomatic (Bolger, Lohse,
143 and Usadel 2014), adaptors were removed, reads were trimmed as soon as the average per-
144 base quality dropped below 20 on 4 nt sliding windows, and reads shorter than 50 bp were
145 discarded, with an additional 10 bp removed from the beginning of read pair one and the end
146 of read pair two to remove the low complexity tail specific to the Accel-NGS 1S Plus kit, per the
147 manufacturer's instruction. Reads were assembled using SPAdes (Bankevich et al. 2012; single-
148 cell option, and k-mers 21, 33, and 55), and the contigs were processed with VirSorter to
149 distinguish viral from microbial contigs (virome decontamination mode; Roux et al. 2015).

150 Contigs that were selected as VirSorter categories 1 and 2 were used to identify dsDNA
151 viral contigs (as in Trubl et al. 2018). ssDNA viruses, due to short genomes and highly divergent
152 hallmark genes, can frequently be missed by automatic viral sequence identification tools (e.g.
153 VirSorter from Roux et al. 2015 or VirFinder in Ren et al. 2017). We therefore applied a two-
154 step approach to ssDNA identification. First, we identified circular contigs that matched ssDNA
155 marker genes from the PFAM database (Viral_Rep and Phage_F domains), using hmmsearch
156 (Eddy, 2009; HMMER v3; cutoffs: score ≥ 50 and e-value ≤ 0.001). This identified four Phage_F-
157 encoding and five Viral_Rep-encoding circular contigs, i.e. presumed complete genomes.
158 Second, 2 new HMM profiles were generated, using the protein sequences from the nine

159 identified circular viral contigs, and used to search (hmmsearch with the same cutoffs) the
160 viromes' predicted proteins. This resulted in a final set of 23 predicted ssDNA contigs identified
161 across nine viromes (Table S1).

162 The viral contigs were clustered at 95% average nucleotide identify (ANI) across 85% of
163 the contig (Roux et al. 2018a) using nucmer (Delcher, Salzberg, and Phillippy 2003). The same
164 contigs were also compared by BLAST to a pool of potential laboratory contaminants (i.e.
165 Enterobacteria phage PhiX17, Alpha3, M13, Cellulophaga baltica phages, and
166 Pseudoalteromonas phages), and any contigs matching a potential contaminant at more than
167 95% ANI across 80% of the contig were removed. Viral operational taxonomic units (vOTUs)
168 were defined as non-redundant (i.e. post-clustering) viral contigs >10kb for dsDNA viruses
169 (from VirSorter categories 1 or 2; Roux et al. 2015) and circular contigs from 4–8 kb for
170 Microviridae viruses or 1–5 kb for circular replication-associated protein (Rep)-encoding ssDNA
171 (CRESS DNA) viruses. The vOTUs represent populations that are likely species-level taxa and
172 there is extensive literature context supporting this new standard terminology, which is
173 summarized in a recent consensus paper (Roux et al. 2018a). The relative abundance of vOTUs
174 was estimated based on post-QC reads mapping at $\geq 90\%$ ANI and covering >10% of the contig
175 (Paez-Espino et al. 2016; Roux et al. 2018a) using Bowtie2 (Langmead and Salzberg 2012).
176 Figures were generated with R, using packages Vegan for diversity (Oksanen et al. 2016) and
177 ggplot2 (Wickham 2016) or pheatmap (Kolde 2012) for heatmaps. Hierarchical clustering
178 (function pvclust; method.dist="euclidean" and method.hclust="complete") was conducted on
179 Bray-Curtis dissimilarity matrices using 1000 bootstrap iterations and only the approximately
180 unbiased (AU) bootstrap values were reported.

181 *Data availability*

182 The 18 viromes from Experiments 1 and 2 are available at the IsoGenie project database
183 under data downloads at <https://isogenie.osu.edu/> and at CyVerse (<https://www.cyverse.org/>)
184 file path /iplant/home/shared/iVirus/Trubl_Soil_Viromes. Data was processed using The Ohio
185 Supercomputer Center (Ohio Supercomputer Center 1987). The final optimized protocol can be
186 accessed here: [https://www.protocols.io/view/soil-viral-extraction-protocol-for-ssdna-amp-](https://www.protocols.io/view/soil-viral-extraction-protocol-for-ssdna-amp-dsdna-tzzep76)
187 [dsdna-tzzep76](https://www.protocols.io/view/soil-viral-extraction-protocol-for-ssdna-amp-dsdna-tzzep76).

188 **Results and Discussion**

189 Two experiments were performed to optimize the generation of quantitatively-
190 amplified viromes from soil samples (Fig. 1). Experiment 1 evaluated three different DNA
191 extraction methods for DNA yield, purity, and successful virome generation on the challenging
192 humic-laden bog and fen soils. Experiment 2 compared two viral particle purification methods
193 (with or without CsCl) and two virion lysis methods (heat vs bead-beating), for DNA yield,
194 microbial DNA contamination, and successful virome generation for all three site habitats
195 (palsa, bog and fen). An optimized virome generation protocol was determined for these palsa,
196 bog and fen soils.

197 *Different DNA extraction methods display variable efficiencies and recover distinct vOTUs*

198 In Experiment 1, three DNA extraction methods were evaluated for DNA yield and
199 purity: PowerSoil DNA extraction kits, Wizard mini columns, and a classic molecular biological
200 approach using cetyl trimethylammonium bromide (CTAB). The PowerSoil kit was designed for
201 humic-rich soils, which dominate our site (Hodgkins et al. 2014; Normand et al. 2017), and has
202 performed well previously for viral samples (Iker et al. 2013). Wizard mini columns were used
203 previously to generate viromes from these soils (Trubl et al. 2018). CTAB performs well on
204 polysaccharide-rich samples (Porebski, Bailey, and Baum 1997), such as our site's peat soils.

205 Overall, the PowerSoil kit performed best, with the highest DNA yields and increased
206 purity which led to more successful libraries and identification of more vOTUs. Specifically, the
207 PowerSoil kit generally yielded the most DNA in the bog and fen, although the increase was
208 only significant in the fen habitat (one-way ANOVA, α 0.05, and Tukey's test with p-value <0.05;
209 Fig. 2A). DNA purity, which is also essential to virome generation (since proteins, phenols, and
210 organics can inhibit amplification; reviewed in Alaeddini 2012), was examined via A260:280 (Fig
211 2B; for proteins and phenol contamination; Maniatis et al. 1982) and A260:230 ratios (Fig 2C;
212 for carbohydrates and phenols; Maniatis et al. 1982; Tanveer, Yadav, and Yadav 2016). We
213 posited that A260:280 is a more robust predictor of virome success, since previous work
214 showed that A260:230 of DNA extracts had limited correlation to amplification success (Costa
215 et al. 2010; Ramos-Gómez et al. 2014), and is highly variable for low DNA concentrations typical
216 for soil viral extracts. For bog samples, at least one replicate from each DNA extraction method
217 had a clean sample based on A260:280 (defined as 1.6–2.1), and PowerSoil extracts consistently
218 exhibited the highest A260:230 ratios (i.e. inferred to be cleanest). For the fen, the same trend
219 was recapitulated (PowerSoil having the cleanest ratios). One bog PowerSoil sample, and one
220 fen CTAB sample, had unusually high A260:280 ratios, suggesting the presence of leftover
221 extraction reagents in the sample.

222 Soil microbial metagenome protocols commonly include further DNA clean-up after
223 extraction to remove inhibitory substances commonly seen in soil (summarized in Roose-
224 Amsaleg, Garnier-Sillam, and Harry 2001; Roslan, Mohamad, and Omar 2017), therefore we
225 evaluated the potential improvement in viral DNA purity from clean-up by AMPure beads.
226 Purity (measured via A260:280) improved significantly in the bog Wizard and PowerSoil
227 extracts, and the fen CTAB extracts, and improved in both bog and fen CTAB and PowerSoil
228 extracts. For A260:230, all post-clean-up DNAs were still below the standard minimum
229 threshold (1.6–2.2, Fig.2C).

230 Although DNA extract yield and purity metrics are useful indicators of extract quality,
231 the goal is successful library preparation and sequencing. Thus, we used the cleaned up DNA to
232 attempt virome generation, which revealed that PowerSoil-derived DNA was more amenable to
233 library construction than the other extracts. Specifically, five of six PowerSoil extracts
234 successfully generated libraries, whereas only one of the Wizard and none of the CTAB extracts
235 led to successful library construction (threshold for success described in methods). Presumably,

236 the success of the PowerSoil extraction methods was increased due to the kit having been
237 optimized for humic-laden soils (specific reagents proprietary to Qiagen).

238 Where sequencing library construction was successful, we then sequenced and analyzed
239 the resultant viromes to assess whether the vOTUs captured varied across replicate PowerSoil
240 viromes and between the PowerSoil and Wizard viromes. In total, the 6 viromes produced
241 1,311 dsDNA viral contigs (VirSorter categories 1 and 2; Roux et al. 2015), which clustered into
242 516 vOTUs (see methods; Roux et al. 2018a). There were dramatic changes in the presence and
243 relative abundance of vOTUs across the two DNA extraction kits evaluated, the biological
244 replicates, and the soil habitats, which is partially the result of uneven coverage due to the 15
245 rounds of PCR performed to amplify the DNA. While PCR amplification is a powerful tool that
246 permits ecological interpretation of resulting viral data (Duhaime and Sullivan 2012; Solonenko
247 and Sullivan 2013; Solonenko et al. 2013), library amplification can lead to an enrichment in
248 short inserts, resulting in uneven coverage, a bias that scales with the number of PCR cycles
249 performed (Roux et al. 2018b). The differences in vOTU presence/absence among viromes
250 decreased but remained noticeable even when using the most sensitive thresholds proposed
251 for the detection of a vOTU in a metagenome (Roux et al. 2018b, Fig. S2). This suggests bias
252 from the DNA extraction method (as reported previously for microbial populations; Delmont et
253 al. 2011; Zielińska et al. 2017), and/or haphazard detection of low-abundance vOTUs due to
254 inadequate sampling and/or sequencing depth.

255 *Heat-based lysis of non-CsCl-purified virus particles provides the most comprehensive viromes*

256 With PowerSoil identified as the optimal DNA extraction kit (yielding the most successful
257 viromes), in Experiment 2 we next evaluated whether density-based particle purification and/or
258 alternative virion lysis methods could increase viral DNA yield, as previously suggested
259 (Delmont et al. 2011; Zielińska et al. 2017). We reasoned that purification by cesium-chloride
260 (CsCl) density gradients could result in viral loss (as previously described in Trubl et al. 2016),
261 but also lead to reduced microbial DNA contamination by removing ultra-small (<0.2µm) cells
262 that survive the filtration step. For lysis methods, we compared the two suggested in the
263 PowerSoil protocol and posited that heat lysis would work better because it has been used
264 previously on viruses (reviewed in McCance 1996) and the bead-beating method was previously
265 shown to cause ~27% more viral loss than not using beads with PowerSoil extraction kit on
266 diverse soils (Iker et al. 2013).

267 To assess this, viruses were resuspended from three palsa, bog, and fen samples as
268 previously described (Trubl et al. 2016), and then the samples were split with half undergoing
269 particle purification via CsCl gradients and half not, and each purification treatment lysed by
270 each of the two lysis methods (heat and bead beating) for a total of 4 treatments, all followed
271 by PowerSoil extraction (Fig. 1). We found significant differences in DNA yield due to
272 purification and lysis method choice (Fig. 4, one-way ANOVA, α 0.05, and Tukey's test with p -
273 value <0.05). CsCl purification had the most impact: yield was higher without it than with it for
274 all but one sample (Palsa, -CsCl[BB]). Lysis method also mattered, with heat producing
275 significantly higher DNA yield than bead-beating (t test, p -value <0.05), for the -CsCl samples in

276 the palsa and fen samples (not significant in the bog) (Fig. 4). These findings suggest that DNA
277 yields are best when not purifying the resuspended viral particles and when lysed using heat.

278 Higher DNA yields could result from contaminating (i.e. non-viral) DNA, so we quantified
279 microbial DNA in all extracts via 16S rRNA gene qPCR (Fig. 5). Surprisingly, we generally
280 observed higher microbial contamination in the CsCl-purified samples (Fig. 5, one-way ANOVA,
281 α 0.05, and Tukey's test with p-value <0.05), and this varied along the thaw gradient with palsa
282 contamination being higher than that of bog and fen samples. Since residual soil organics can
283 interfere with PCR (Kontanis and Reed, 2006), we repeated the qPCR assay after DNA
284 purification with the PowerClean kit. Generally, microbial contamination increased for -CsCl
285 samples (Fig. 5), suggesting that their previously low microbial contamination was due to PCR
286 inhibition, and +CsCl samples had mixed results, but in each habitat +CsCl[BB] samples had a
287 significant increase in measurable contamination (Fig. 5). All treatments had higher qPCR-based
288 microbial contamination after PowerClean, except +CsCl[H] samples which averaged a 1.5–26-
289 fold reduction. Overall there was still no consistent, or significant, improvement in microbial
290 contamination from inclusion of a CsCl purification step, even after PowerClean treatment.

291 Since we sequenced bog and fen viromes to characterize treatment effects on viral
292 signal in Experiment 1, we opted in Experiment 2 to do this evaluation on the 12 Palsa samples,
293 which were all sequenced. We found that the higher DNA yields in the -CsCl samples led to ~3-
294 fold more viral contigs, which were also an average of 2.3-fold larger than +CsCl samples (Fig.
295 6A). The results from heat-lysis samples were more modest as they resulted in only ~33% more
296 viral contigs, and statistically indistinguishable contig sizes across treatments (Fig. 6B; unequal
297 variance t-test, p-value >0.05). These findings suggest that the optimal combination for
298 recovering virus genomes from these soils is to skip CsCl purification and lyse the resultant viral
299 particles using heat.

300 We next evaluated whether vOTU representation and diversity estimates from the same
301 samples varied across the purification and lysis methods tested here. In total, we identified 66
302 vOTUs from these 12 palsa viromes, with 100% of the vOTUs identified in -CsCl samples, 89%
303 (59) identified in the +CsCl samples, and vOTUs identified by both datasets displaying an
304 average of 30-fold more coverage (Fig. 7) in -CsCl viromes. This indicates that the CsCl
305 purification step reduced the samples to a subset of the initial viral community and did not help
306 recover virus genomes that would be missed otherwise. Profiles of the recovered communities
307 clustered first by soil core (AU branch supports >76), then mostly by purification (AU branch
308 supports >66), and lastly by lysis, and did not change after varying the threshold for considering
309 a lineage present (Fig. S3). Collectively this suggests that differences introduced by sample
310 preparation were outweighed by the distinctiveness of each core's viral community. We
311 proceeded to use diversity metrics to evaluate the different methods' impacts. The alpha
312 diversity metrics paralleled treatment DNA yields where -CsCl samples were on average 56%
313 more diverse than the +CsCl samples, and heat samples were on average 83% more diverse
314 than the bead-beating samples (Fig. S4A). A comparison of dissimilarities among samples
315 suggested the lysis method had more of an impact, although this effect was variable between
316 samples and thus not statistically significant overall (Fig. S4B).

317 ssDNA viruses are recovered in all 3 habitats

318 Viromes have previously either neglected ssDNA viruses or qualitatively described them,
319 but with the onset of the Accel-NGS 1S Plus kit, we leveraged the viromics data produced here
320 to investigate the diversity and relative abundance of ssDNA viruses in our soil samples. ssDNA
321 viruses are known from culture collections to commonly infect plants as opposed to bacteria,
322 but their distributions in nature remain poorly explored outside of aquatic systems (Labonté
323 and Suttle 2013). Notably, the first quantitative ssDNA/dsDNA viromes suggested that
324 identifiable ssDNA viruses represent a few percent of the viruses observed in marine and
325 freshwater systems (Roux et al. 2016).

326 To assess this biological signal in soils, we investigated the recovery and relative
327 abundance of ssDNA viruses across our different soil habitats and sample preparations. Overall,
328 we identified 35 putative ssDNA viruses, 11 from the Microviridae family and 24 CRESS DNA
329 viruses (Fig. 8), which clustered into 13 vOTUs (3 Microviridae and 10 CRESS DNA). These ssDNA
330 vOTUs were only a small fraction of the total vOTUs identified in each habitat (1% in bog and
331 fen, and 8% in palsa) and only bog and fen samples included both types (Microviridae and
332 CRESS-DNA), while palsa samples included exclusively CRESS-DNA viruses (Table S1). This
333 suggests that, as for dsDNA viruses, the composition of the ssDNA virus community varies along
334 the thaw gradient, potentially as a result of known changes in the host communities (Trubl et
335 al. 2018), both microbial (Mondav et al. 2017; Woodcroft et al. 2018) and plant (Hodgkins et al.
336 2014; Normand et al. 2017). Notably, bead-beating-lysis samples did not include any ssDNA
337 viruses. We posit that this was likely due to the heterogeneity of soil, because ssDNA viruses
338 have previously been identified from experiments that used a bead-beating lysis (Hopkins et al.
339 2014). Finally, ssDNA viruses represented on average 4% of the community in the samples
340 where ssDNA and dsDNA viruses were detected, which suggests that ssDNA viruses are not the
341 dominant type of virus in these soils.

342 Conclusions

343 The development of a sample-to-sequence pipeline for ssDNA and dsDNA viruses in soils
344 is crucial for characterizing viruses and their impact in these ecosystems. Our work here built
345 upon previous work that optimized virus resuspension from soils by evaluating DNA extraction
346 and lysis methods to increase DNA yields and purity. Additionally, this is the first evaluation of
347 the Accel-NGS 1S Plus kit to capture ssDNA viruses in soils. Although these efforts have made
348 inroads towards characterizing the soil virosphere, several challenges remain. Initial challenges
349 arise from lack of data on which fraction of the free virus particles are being recovered from
350 soils, and how to achieve a holistic sampling of the virus community (i.e. dsDNA, ssDNA, and
351 RNA viruses). Beyond these, the presence of non-viral DNA in capsids or vesicles, e.g. gene
352 transfer agents, can dilute viral signal in viromes and complicate interpretation (reviewed in
353 Roux et al. 2013; Hurwitz, Hallam and Sullivan 2013; Lang and Beatty 2010), although new
354 methods are being developed to identify and characterize these contaminating agents
355 (reviewed in Lang, Westbye, Beatty 2017). The advent of long-read sequencing technologies

356 have recently been applied to viromics and can improve contig generation for regions of
357 genome with high similarity or complexity (summarized in Roux et al. 2017; Karamitros et al.
358 2018) and prevent formation of chimeric contigs. Longer-read viromes can thereby not only
359 increase vOTU recovery but also provide resolution of hypervariable genome regions with
360 niche-defining genes, and help capture micro-diverse populations missed by short-read
361 assemblies (Warwick-Dugdale et al. 2018). Next, inferences of viral impacts on microbial
362 communities and C cycling will require predicting hosts both in silico (Edwards et al. 2015; Paez-
363 Espino et al. 2017) and in vitro (Deng et al. 2014; Brum & Sullivan 2015; Cenens et al. 2015),
364 approaches to which are emerging. Finally, identification of the active viral community and
365 characterization of their roles in biogeochemical processes can be better resolved with
366 techniques like stable isotope-based approaches linked with nanoscale secondary ion mass
367 spectrometry (NanoSIP; Pacton et al. 2014; Pasulka et al. 2018; Gates et al. 2018). Application
368 of these and other approaches to soil viromics will increase and diversify publicly available viral
369 datasets, advance our understanding of soil viral ecology, and improve our knowledge of viral
370 roles in soil ecosystems.

371

372 Acknowledgments

373 We thank Olivier Zablocki for his suggestions and comments. We thank Moira Hough, Sky
374 Dominguez, and Nicole Raab for collecting the soil cores and geochemical data, and the Abisko
375 Naturvetenskapliga Station for field support. Bioinformatics were supported by The Ohio
376 Supercomputer Center and by the National Science Foundation under Award Numbers DBI-
377 0735191 and DBI-1265383; URL: www.cyverse.org. This study was funded by the Genomic
378 Science Program of the United States Department of Energy Office of Biological and
379 Environmental Research (grants DE-SC0010580 and DE-SC0016440), The Office of Science,
380 Office of Workforce Development for Teachers and Scientists, Office of Science Graduate
381 Student Research (SCGSR) program, and by the Gordon and Betty Moore Foundation
382 Investigator Award (GBMF#3790 to MBS). The SCGSR program is administered by the Oak Ridge
383 Institute for Science and Education (ORISE) for the DOE. ORISE is managed by ORAU under
384 contract number DE-SC0014664.

385 References

- 386 Alaeddini, R., 2012. Forensic implications of PCR inhibition—a review. *Forensic Science*
387 *International: Genetics*, 6(3), pp.297-305.
- 388 Amgarten, D.E., Braga, L.P.P., Da Silva, A.M. and Setubal, J.C., 2018. MARVEL, a Tool for
389 Prediction of Bacteriophage Sequences in Metagenomic Bins. *Frontiers in genetics*, 9,
390 p.304.
- 391 Bankevich, A., Nurk, S., Antipov, D., Gurevich, A.A., Dvorkin, M., Kulikov, A.S., Lesin, V.M.,
392 Nikolenko, S.I., Pham, S., Prjibelski, A.D. and Pyshkin, A.V., 2012. SPAdes: a new genome

- 393 assembly algorithm and its applications to single-cell sequencing. *Journal of*
394 *computational biology*, 19(5), pp.455-477.
- 395 Binga, E.K., Lasken, R.S. and Neufeld, J.D., 2008. Something from (almost) nothing: the impact
396 of multiple displacement amplification on microbial ecology. *The ISME journal*, 2(3),
397 p.233
- 398 Bolger, A.M. Lohse, M. and Usadel, B. 2014. Trimmomatic: a flexible trimmer for Illumina
399 sequence data. *Bioinformatics*, p.btu170.
- 400 Brum, J.R. and Sullivan, M.B., 2015. Rising to the challenge: accelerated pace of discovery
401 transforms marine virology. *Nature Reviews Microbiology*, 13(3), p.147.
- 402 Cenens, W., Makumi, A., Govers, S.K., Lavigne, R. and Aertsen, A., 2015. Viral transmission
403 dynamics at single-cell resolution reveal transiently immune subpopulations caused by a
404 carrier state association. *PLoS genetics*, 11(12), p.e1005770.
- 405 Costa, J., Mafra, I., Amaral, J.S. and Oliveira, M.B.P., 2010. Detection of genetically modified
406 soybean DNA in refined vegetable oils. *European Food Research and Technology*,
407 230(6), pp.915-923.
- 408 Delcher, A.L., Salzberg, S.L. and Phillippy, A.M., 2003. Using MUMmer to identify similar regions
409 in large sequence sets. *Current protocols in bioinformatics*, (1), pp.10-3.
- 410 Delmont, T.O., Robe, P., Cecillon, S., Clark, I.M., Constancias, F., Simonet, P., Hirsch, P.R. and
411 Vogel, T.M., 2011. Accessing the soil metagenome for studies of microbial diversity.
412 *Applied and Environmental Microbiology*, 77(4), pp.1315-1324.
- 413 Deng, L., Ignacio-Espinoza, J.C., Gregory, A.C., Poulos, B.T., Weitz, J.S., Hugenholtz, P. and
414 Sullivan, M.B., 2014. Viral tagging reveals discrete populations in *Synechococcus* viral
415 genome sequence space. *Nature*, 513(7517), p.242.
- 416 Duhaime, M.B. and Sullivan, M.B., 2012. Ocean viruses: rigorously evaluating the metagenomic
417 sample-to-sequence pipeline. *Virology*, 434(2), pp.181-186.
- 418 Eddy, S.R., 2009. A new generation of homology search tools based on probabilistic inference.
419 In *Genome Informatics 2009: Genome Informatics Series Vol. 23* (pp. 205-211).
- 420 Edwards, R.A., McNair, K., Faust, K., Raes, J. and Dutilh, B.E., 2015. Computational approaches
421 to predict bacteriophage–host relationships. *FEMS microbiology reviews*, 40(2), pp.258-
422 272.
- 423 Fierer, N., 2017. Embracing the unknown: disentangling the complexities of the soil
424 microbiome. *Nature Reviews Microbiology*, 15(10), p.579.
- 425 Gates, S.D., Condit, R.C., Moussatche, N., Stewart, B.J., Malkin, A.J. and Weber, P.K., 2018. High
426 Initial Sputter Rate Found for Vaccinia Virions Using Isotopic Labeling, NanoSIMS, and
427 AFM. *Analytical chemistry*, 90(3), pp.1613-1620.
- 428 Han, L., Sun, K., Jin, J. and Xing, B., 2016. Some concepts of soil organic carbon characteristics
429 and mineral interaction from a review of literature. *Soil Biology and Biochemistry*, 94,
430 pp.107-121.
- 431 Hayes, S., Mahony, J., Nauta, A. and van Sinderen, D., 2017. Metagenomic approaches to assess
432 bacteriophages in various environmental niches. *Viruses*, 9(6), p.127.

- 433 Hodgkins, S.B., Tfaily, M.M., McCalley, C.K., Logan, T.A., Crill, P.M., Saleska, S.R., Rich, V.I. and
434 Chanton, J.P., 2014. Changes in peat chemistry associated with permafrost thaw
435 increase greenhouse gas production. *Proceedings of the National Academy of Sciences*,
436 p.201314641.
- 437 Hopkins, M., Kailasan, S., Cohen, A., Roux, S., Tucker, K.P., Shevenell, A., Agbandje-McKenna, M.
438 and Breitbart, M., 2014. Diversity of environmental single-stranded DNA phages
439 revealed by PCR amplification of the partial major capsid protein. *The ISME journal*,
440 8(10), p.2093
- 441 Hurwitz, B.L., Hallam, S.J. and Sullivan, M.B., 2013. Metabolic reprogramming by viruses in the
442 sunlit and dark ocean. *Genome biology*, 14(11), p.R123.
- 443 Iker, B.C., Bright, K.R., Pepper, I.L., Gerba, C.P. and Kitajima, M., 2013. Evaluation of commercial
444 kits for the extraction and purification of viral nucleic acids from environmental and
445 fecal samples. *Journal of virological methods*, 191(1), pp.24-30.
- 446 Johansson, T., Malmer, N., Crill, P.M., Friborg, T., Aakerman, J.H., Mastepanov, M. and
447 Christensen, T.R., 2006. Decadal vegetation changes in a northern peatland, greenhouse
448 gas fluxes and net radiative forcing. *Global Change Biology*, 12(12), pp.2352-2369.
- 449 Karamitros, T., van Wilgenburg, B., Wills, M., Klenerman, P. and Magiorkinis, G., 2018.
450 Nanopore sequencing and full genome de novo assembly of human cytomegalovirus
451 TB40/E reveals clonal diversity and structural variations. *BMC genomics*, 19(1), p.577.
- 452 Karlsson, O.E., Belák, S. and Granberg, F., 2013. The effect of preprocessing by sequence-
453 independent, single-primer amplification (SISPA) on metagenomic detection of viruses.
454 *Biosecurity and bioterrorism: biodefense strategy, practice, and science*, 11(S1),
455 pp.S227-S234
- 456 Kim, M.S., Whon, T.W. and Bae, J.W., 2013. Comparative viral metagenomics of environmental
457 samples from Korea. *Genomics & informatics*, 11(3), pp.121-128.
- 458 Kolde, R., 2012. Pheatmap: pretty heatmaps. R package version, 61
- 459 Kontanis, E.J. and Reed, F.A., 2006. Evaluation of real-time PCR amplification efficiencies to
460 detect PCR inhibitors. *Journal of forensic sciences*, 51(4), pp.795-804.
- 461 Labonté, J.M. and Suttle, C.A., 2013. Previously unknown and highly divergent ssDNA viruses
462 populate the oceans. *The ISME journal*, 7(11), p.2169.
- 463 Lang, A.S., Westbye, A.B. and Beatty, J.T., 2017. The distribution, evolution, and roles of gene
464 transfer agents in prokaryotic genetic exchange. *Annual review of virology*, 4, pp.87-104.
- 465 Langmead, B. and Salzberg, S.L., 2012. Fast gapped-read alignment with Bowtie 2. *Nature*
466 *methods*, 9(4), p.357.
- 467 Lehmann, J. and Kleber, M., 2015. The contentious nature of soil organic matter. *Nature*,
468 528(7580), p.60.
- 469 Maniatis T., Fritsch E.F., Sambrook J. *Molecular cloning: a laboratory manual*. Cold Spring
470 Harbor: Cold Spring Harbor Laboratory; 1982.
- 471 Marine, R., McCarren, C., Vorrasane, V., Nasko, D., Crowgey, E., Polson, S.W. and Wommack,
472 K.E., 2014. Caught in the middle with multiple displacement amplification: the myth of

- 473 pooling for avoiding multiple displacement amplification bias in a metagenome.
474 *Microbiome*, 2(1), p.3
- 475 Mondav, R., McCalley, C.K., Hodgkins, S.B., Froking, S., Saleska, S.R., Rich, V.I., Chanton, J.P. and
476 Crill, P.M., 2017. Microbial network, phylogenetic diversity and community membership
477 in the active layer across a permafrost thaw gradient. *Environmental microbiology*,
478 19(8), pp.3201-3218
- 479 Narayan, A., Jain, K., Shah, A.R. and Madamwar, D., 2016. An efficient and cost-effective
480 method for DNA extraction from athalassohaline soil using a newly formulated cell
481 extraction buffer. *3 Biotech*, 6(1), p.62.
- 482 Narr, A., Nawaz, A., Wick, L.Y., Harms, H. and Chatzinotas, A., 2017. Soil Viral Communities Vary
483 Temporally and along a Land Use Transect as Revealed by Virus-Like Particle Counting
484 and a Modified Community Fingerprinting Approach (fRAPD). *Frontiers in microbiology*,
485 8, p.1975.
- 486 Normand, A.E., Smith, A.N., Clark, M.W., Long, J.R. and Reddy, K.R., 2017. Chemical composition
487 of soil organic matter in a subarctic peatland: influence of shifting vegetation
488 communities. *Soil Science Society of America Journal*, 81(1), pp.41-49.
- 489 Ohio Supercomputer Center. 1987. Ohio Supercomputer Center. Columbus OH: Ohio
490 Supercomputer Center.
- 491 Oksanen, J., Blanchet, F., Kindt, R., Legendre, P. and O'Hara, R., 2016. *Vegan: community
492 ecology package*. R package 2.3-3.
- 493 Olefeldt, D., Roulet, N.T., Bergeron, O., Crill, P., Bäckstrand, K. and Christensen, T.R., 2012. Net
494 carbon accumulation of a high-latitude permafrost palsa mire similar to permafrost-free
495 peatlands. *Geophysical Research Letters*, 39(3).
- 496 Pacton, M., Wacey, D., Corinaldesi, C., Tangherlini, M., Kilburn, M.R., Gorin, G.E., Danovaro, R.
497 and Vasconcelos, C., 2014. Viruses as new agents of organomineralization in the
498 geological record. *Nature communications*, 5, p.4298.
- 499 Paez-Espino, D., Eloë-Fadrosh, E.A., Pavlopoulos, G.A., Thomas, A.D., Huntemann, M.,
500 Mikhailova, N., Rubin, E., Ivanova, N.N. and Kyrpides, N.C., 2016. Uncovering Earth's
501 virome. *Nature*, 536(7617), p.425.
- 502 Paez-Espino, D., Pavlopoulos, G.A., Ivanova, N.N. and Kyrpides, N.C., 2017. Nontargeted virus
503 sequence discovery pipeline and virus clustering for metagenomic data. *nature
504 protocols*, 12(8), p.1673.
- 505 Pasulka, A.L., Thamatrakoln, K., Kopf, S.H., Guan, Y., Poulos, B., Moradian, A., Sweredoski, M.J.,
506 Hess, S., Sullivan, M.B., Bidle, K.D. and Orphan, V.J., 2018. Interrogating marine
507 virus-host interactions and elemental transfer with BONCAT and nanoSIMS-based
508 methods. *Environmental microbiology*, 20(2), pp.671-692.
- 509 Phan, T.G., Mori, D., Deng, X., Rajindrajith, S., Ranawaka, U., Ng, T.F.F., Bucardo-Rivera, F.,
510 Orlandi, P., Ahmed, K. and Delwart, E., 2015. Small circular single stranded DNA viral
511 genomes in unexplained cases of human encephalitis, diarrhea, and in untreated
512 sewage. *Virology*, 482, pp.98-104

- 513 Porebski, S., Bailey, L.G. and Baum, B.R., 1997. Modification of a CTAB DNA extraction protocol
514 for plants containing high polysaccharide and polyphenol components. *Plant molecular*
515 *biology reporter*, 15(1), pp.8-15
- 516 Ramos-Gómez, S., Busto, M.D., Perez-Mateos, M. and Ortega, N., 2014. Development of a
517 method to recovery and amplification DNA by real-time PCR from commercial vegetable
518 oils. *Food Chemistry*, 158, pp.374-383.
- 519 Ren, J., Ahlgren, N.A., Lu, Y.Y., Fuhrman, J.A. and Sun, F., 2017. VirFinder: a novel k-mer based
520 tool for identifying viral sequences from assembled metagenomic data. *Microbiome*,
521 5(1), p.69.
- 522 Roose-Amsaleg, C.L., Garnier-Sillam, E. and Harry, M., 2001. Extraction and purification of
523 microbial DNA from soil and sediment samples. *Applied Soil Ecology*, 18(1), pp.47-60.
- 524 Rosario, K., Fierer, N., Miller, S., Luongo, J. and Breitbart, M., 2018. Diversity of DNA and RNA
525 viruses in indoor air as assessed via metagenomic sequencing. *Environmental science &*
526 *technology*, 52(3), pp.1014-1027.
- 527 Roslan, M.A.M., Mohamad, M.A.N. and Omar, S.M., 2017. High quality DNA from peat soil for
528 metagenomic studies a minireview on dna extraction methods. *Science*, 1(2), pp.01-06.
- 529 Roux, S., Emerson, J.B., Eloë-Fadrosh, E.A. and Sullivan, M.B., 2017. Benchmarking viromics: an
530 in silico evaluation of metagenome-enabled estimates of viral community composition
531 and diversity. *PeerJ*, 5, p.e3817.
- 532 Roux, S., Krupovic, M., Debroas, D., Forterre, P. and Enault, F., 2013. Assessment of viral
533 community functional potential from viral metagenomes may be hampered by
534 contamination with cellular sequences. *Open biology*, 3(12), p.130160.
- 535 Roux, S., Adriaenssens, E.M., Dutilh, B.E., Koonin, E.V., Kropinski, A.M., Krupovic, M., Kuhn, J.H.
536 Lavigne, R., Brister, J.R., Varsani, A., Amid, C., Aziz, R.K., Bordenstein, S.R., Bork, P.,
537 Breitbart, M., Cochrane, G.R., Daly, R.A., Desnues, C., Duhaime, M.B., Emerson, J.B.,
538 Enault, F., Fuhrman, J.A., Hingamp, P., Hugenholtz, P., Hurwitz, B.L., Ivanova, N.N.,
539 Labonté, J.M., Lee, K-B., Malmstrom, R.R., Martinez-Garcia, M., Mizrachi, I.K., Ogata, H.,
540 Páez-Espino, D., Petit, M-A., Putonti, C., Rattei, T., Reyes, A., Rodriguez-Valera, F.,
541 Rosario, K., Schriml, L., Schulz, F., Steward, G.F., Sullivan, M.S., Sunagawa, S., Suttle, C.A.,
542 Temperton, B., Tringe, S.G., Thurber, R.V., Webster, N.S., Whiteson, K.L., Wilhelm, S.W.,
543 Wommack, K.E., Woyke, T., Wrighton, K.C., Yilmaz, P., Yoshida, T., Young, M.J., Yutin, N.,
544 Allen, L.Z., Kyrpides, N.C., Eloë-Fadrosh, E.A. 2018a. Minimum Information about an
545 Uncultivated Virus Genome (MIUViG). *Nature Biotechnology*, 37(1), 29–37.
- 546 Roux, S., Trubl, G., Goudeau, D., Nath, N., Couradeau, E., Ahlgren, N.A., Zhan, Y., Marsan, D.,
547 Chen, F., Fuhrman, J.A. and Northen, T.R., 2018b. Optimizing de novo genome assembly
548 from PCR-amplified metagenomes (No. e27453v1). *PeerJ Preprints*. Roux, S., Solonenko,
549 N.E., Dang, V.T., Poulos, B.T., Schwenck, S.M., Goldsmith, D.B., Coleman, M.L., Breitbart,
550 M. and Sullivan, M.B., 2016. Towards quantitative viromics for both double-stranded
551 and single-stranded DNA viruses. *PeerJ*, 4, p.e2777.
- 552 Roux, S., Enault, F., Hurwitz, B.L. and Sullivan, M.B., 2015. VirSorter: mining viral signal from
553 microbial genomic data. *PeerJ*, 3, p.e985 Segobola, J., Adriaenssens, E., Tsekoa, T.,

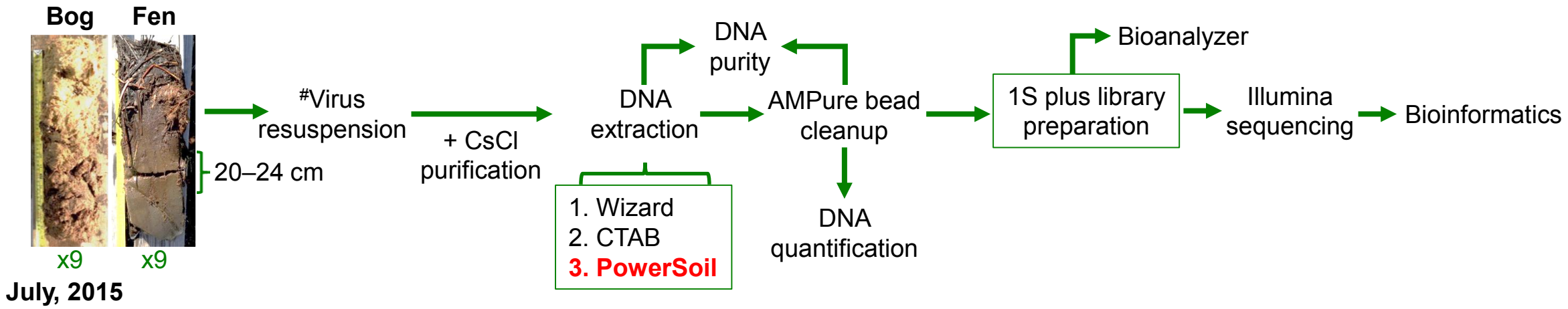
- 554 Rashamuse, K. and Cowan, D., 2018. Exploring viral diversity in a unique South African
555 soil habitat. *Scientific reports*, 8(1), p.111.
- 556 Solonenko, S.A., Ignacio-Espinoza, J.C., Alberti, A., Cruaud, C., Hallam, S., Konstantinidis, K.,
557 Tyson, G., Wincker, P. and Sullivan, M.B., 2013. Sequencing platform and library
558 preparation choices impact viral metagenomes. *BMC genomics*, 14(1), p.320.
- 559 Solonenko, S.A. and Sullivan, M.B., 2013. Preparation of metagenomic libraries from naturally
560 occurring marine viruses. In *Methods in enzymology* (Vol. 531, pp. 143-165). Academic
561 Press.
- 562 Tanveer, A., Yadav, S. and Yadav, D., 2016. Comparative assessment of methods for
563 metagenomic DNA isolation from soils of different crop growing fields. *3 Biotech*, 6(2),
564 p.220.
- 565 Warwick-Dugdale, J., Solonenko, N., Moore, K., Chittick, L., Gregory, A.C., Allen, M.J., Sullivan,
566 M.B. and Temperton, B., 2018. Long-read metagenomics reveals cryptic and abundant
567 marine viruses. *bioRxiv*, p.345041.
- 568 Wickham, H., 2016. *ggplot2: elegant graphics for data analysis*. Springer.
- 569 Wommack, K.E., Bhavsar, J., Polson, S.W., Chen, J., Dumas, M., Srinivasiah, S., Furman, M.,
570 Jamindar, S. and Nasko, D.J., 2012. VIROME: a standard operating procedure for analysis
571 of viral metagenome sequences. *Stand Genomic Sci* 6: 427–439.
- 572 Woodcroft, B.J., Singleton, C.M., Boyd, J.A., Evans, P.N., Emerson, J.B., Zayed, A.A., Hoelzle,
573 R.D., Lamberton, T.O., McCalley, C.K., Hodgkins, S.B. and Wilson, R.M., 2018. Genome-
574 centric view of carbon processing in thawing permafrost. *Nature*, p.1.
- 575 Yilmaz, S., Allgaier, M. and Hugenholtz, P., 2010. Multiple displacement amplification
576 compromises quantitative analysis of metagenomes. *Nature methods*, 7(12), p.943.
- 577 Zielińska, S., Radkowski, P., Blendowska, A., Ludwig-Gałęzowska, A., Łoś, J.M. and Łoś, M., 2017.
578 The choice of the DNA extraction method may influence the outcome of the soil
579 microbial community structure analysis. *MicrobiologyOpen*, 6(4), p.e00453.

Figure 1(on next page)

Overview of experiments to optimize methods for virome generation.

Two experiments (Experiment 1 in green and Experiment 2 in blue) evaluated three DNA extraction methods, two different virion lysis methods, and CsCl virion purification, for optimizing virome generation from three peats soils along a permafrost thaw gradient. Nine soil cores were collected in July 2015, three from each habitat, and used to create 18 samples (9 bog and 9 fen) with 10 ± 1 g of soil in each sample for Experiment 1 and 36 samples (12 palsa, 12 bog, and 12 fen) with 7.5 ± 1 g of soil in each sample for Experiment 2; representative photos of cores were taken by Gary Trubl. Viruses were resuspended as previously described in Trubl et al. (2016), but with the addition of a DNase step and a 1.3 g/ml layer for CsCl purification. Red font color indicates the best-performing option within each set. # denotes adapted protocol from Trubl et al. 2016. ## indicates that only 12 palsa samples proceeded to library preparation.

Experiment 1: identify best DNA extraction method



Experiment 2: increase viral DNA and contig yield

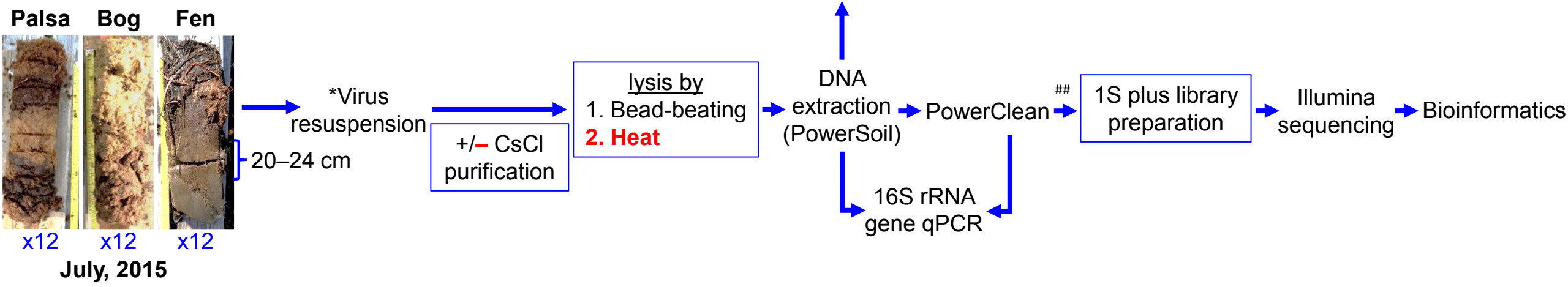


Figure 2(on next page)

Impact of extraction methods on DNA yields and purity (Experiment 1).

Bog samples are shown on the left of each panel, fen samples on the right. DNA extraction methods are color-coded: purple for CTAB, blue for Wizard, and green for PowerSoil. * denotes significant difference via one-way ANOVA, α 0.05, and Tukey's test with p-value <0.05. † denotes significant difference for t test, p-value <0.05; †† = p-value <0.01; ††† = p-value <0.001. A) The DNA concentration (ng/ μ l) after AMPure purification for the three DNA extraction methods. B) DNA extract purity via A260/A280. Dotted lines are purity thresholds: Acceptable range in yellow shading and preferred range in red shading. C) DNA extract purity via A260/A230.

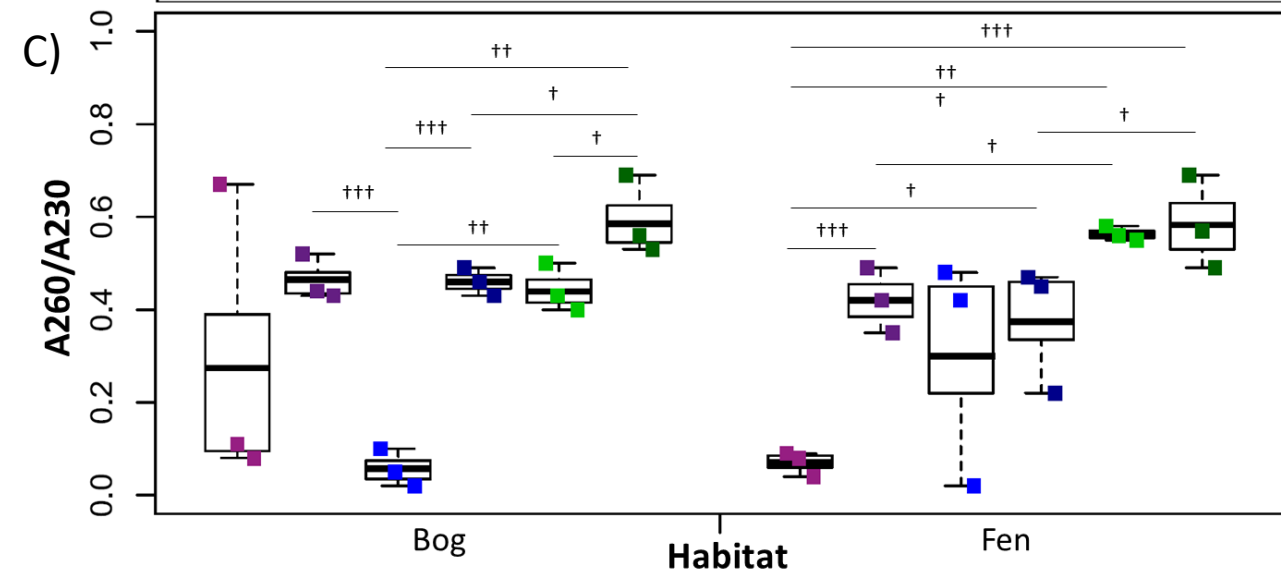
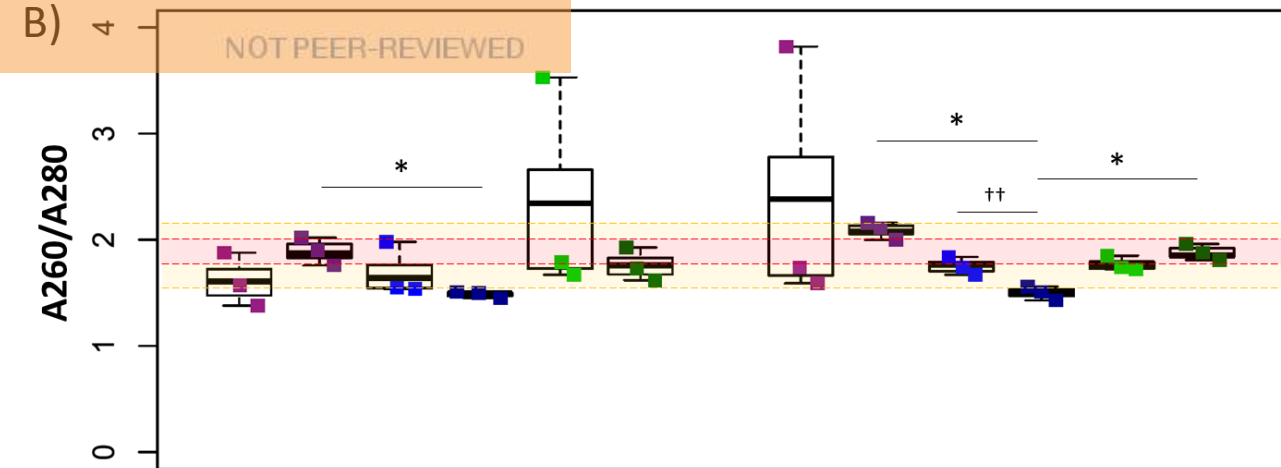
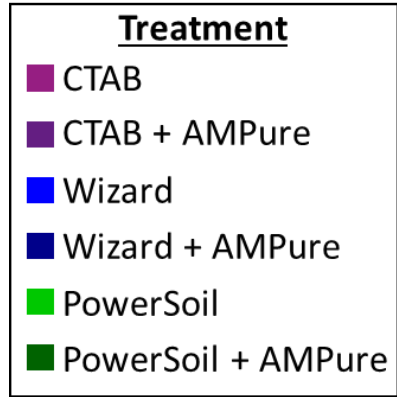
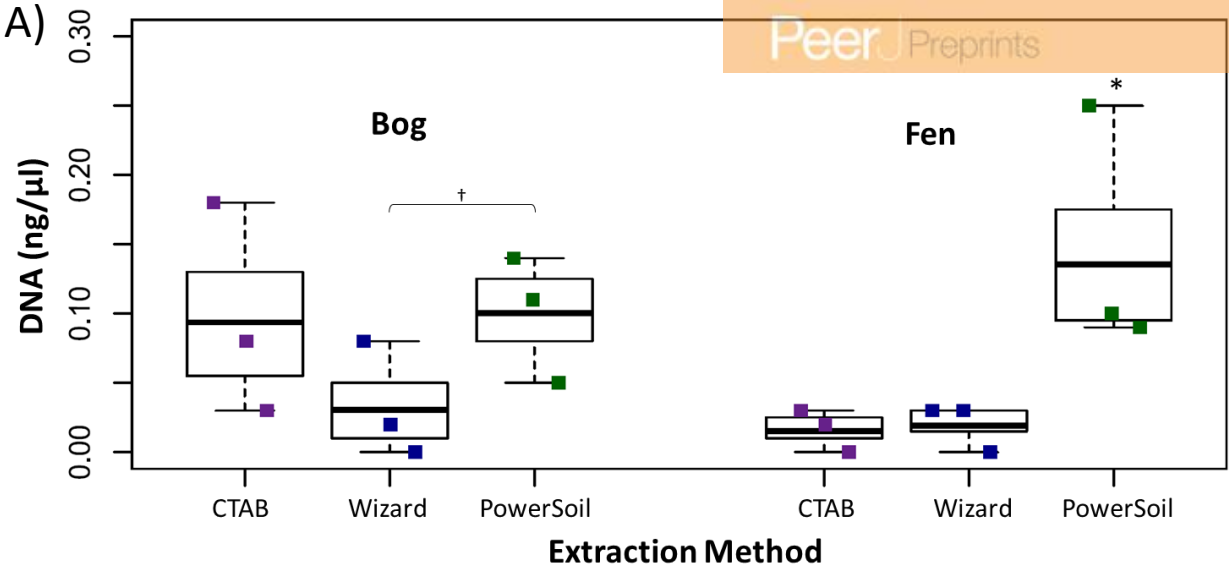
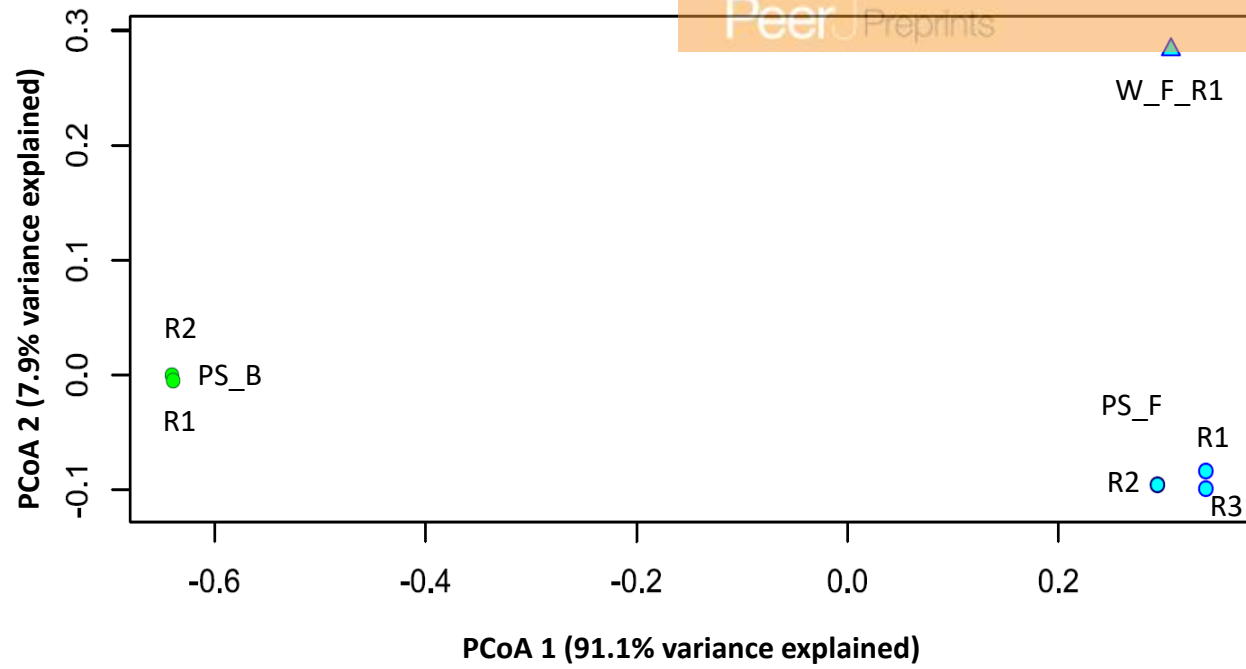


Figure 3(on next page)

Impact of extraction methods on recovery and abundance of vOTUs (Experiment 1).

A principal coordinate analysis of the viromes by normalized relative abundance of the 516 vOTUs based on their Bray-Curtis dissimilarity. Viromes distinguished by habitat (bog colored green, fen blue) and DNA extraction method (PowerSoil as circle, Wizard as triangle).

A)

**Nomenclature**

PS=PowerSoil

W=Wizard

B=Bog

F=Fen

R1/R2/R3=Replicate

Figure 4(on next page)

Impact of lysis and purification methods on DNA yields (Experiment 2).

The DNA concentration (ng/ μ l) is given for the two virion lysis methods used, with or without CsCl purification, for all three habitats. The four treatments are color coded with blue for bead-beating, red for heat lysis and a darker shade if also purified with CsCl. * denotes significant difference via one-way ANOVA, α 0.05, and Tukey's test with p-value <0.05. # denotes n=2. N/D denotes non-detectable DNA concentration.

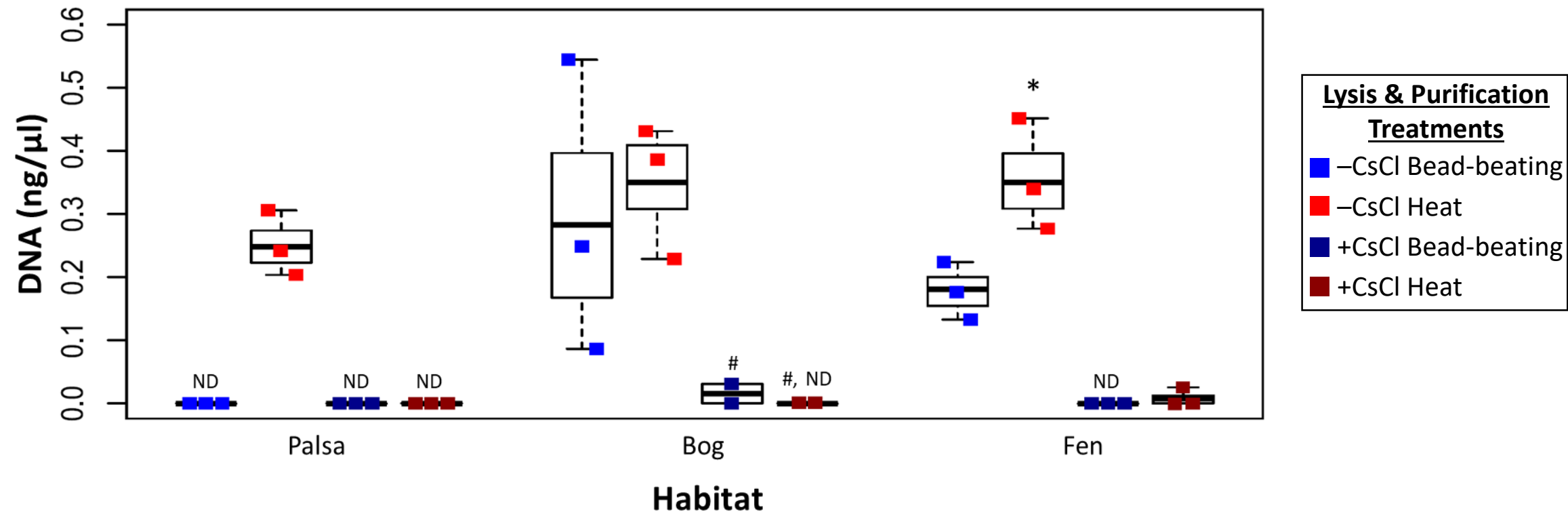


Figure 5(on next page)

Evaluation of microbial contamination (Experiment 2).

The 16S rRNA gene contamination (square root) is indicated for each virome grouped by habitat before (left) and after (right) clean up with PowerClean. The four treatments are color coded with blue for bead-beating and red for heat lysis and a darker shade after CsCl purification. # denotes no data available. 16S qPCR primers were 1406F-1525R (Woodcroft et al. 2018). [†] denotes significant difference for t test, p-value <0.05; ^{††} = p-value <0.01; ^{†††} = p-value <0.001.

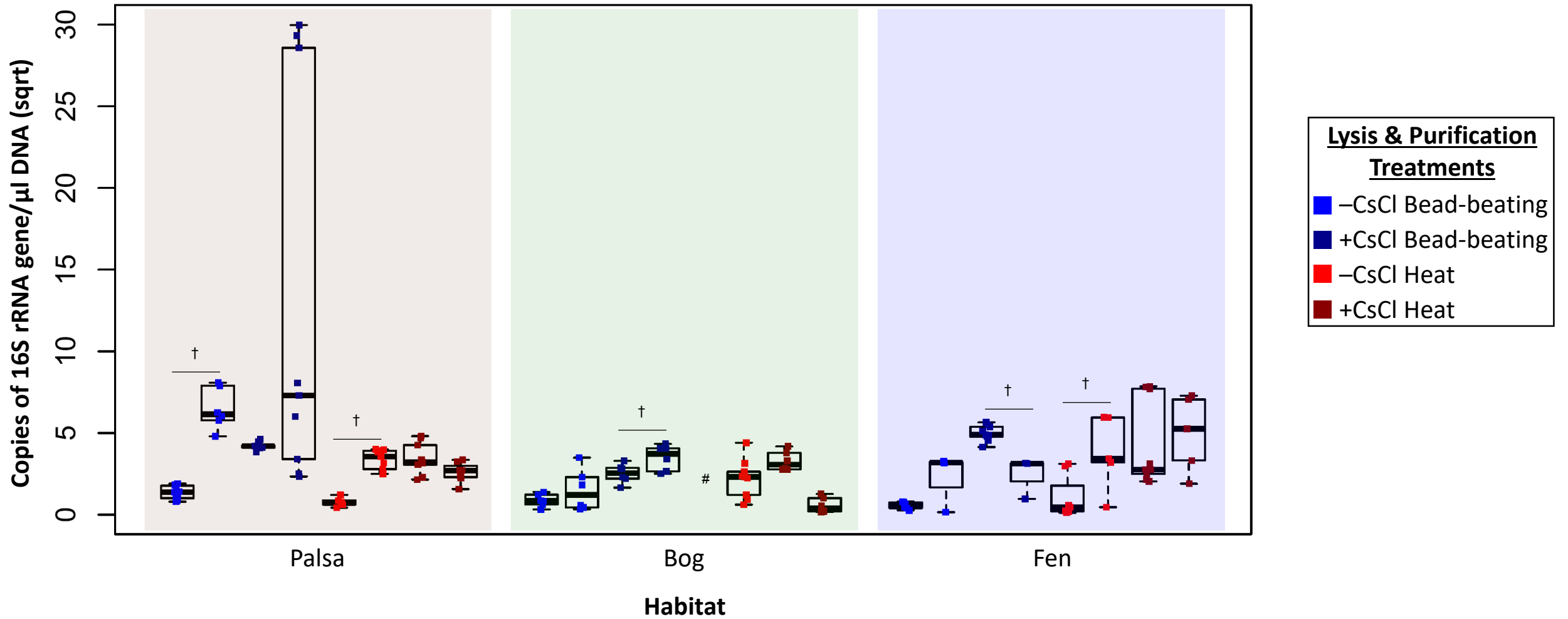


Figure 6(on next page)

Number and size of assembled viral contigs (Experiment 2).

Boxplots show the number of viral contigs assembled, and those > 10 kb, for each treatment. Viral contigs were identified by two approaches: the “conservative” one included only contigs in VirSorter categories 1 & 2 for which a viral origin is very likely, while the “sensitive” one also included contigs in VirSorter category 3, for which a viral origin is possible but unsure.

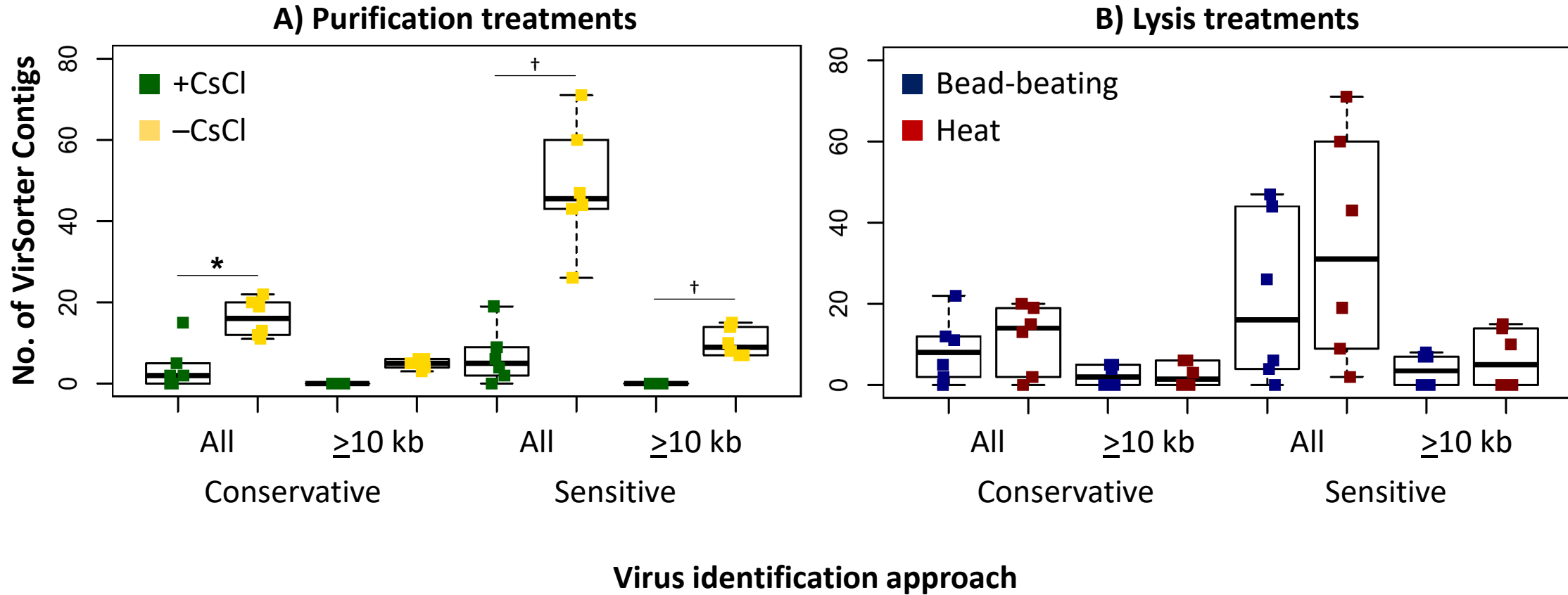


Figure 7 (on next page)

Relative abundance of vOTUs across 12 palsa viromes (Experiment 2).

A heatmap showing the Euclidean-based hierarchical clustering of a Bray-Curtis dissimilarity matrix calculated from vOTU relative abundances within each virome with an approximately unbiased (AU) bootstrap value ($n=1000$). The relative abundances were normalized by contig length and per Gbp of metagenome and were \log_{10} transformed. Reads were mapped to contigs at $\geq 90\%$ nucleotide identity and the relative abundance was set to 0 if reads covered $<10\%$ of the contig. Heatmaps with alternative genome coverage thresholds are presented in Fig. S3. Abbreviations: H, heat lysis; BB, bead-beating; +/- CsCl, with or without cesium chloride purification; C, core.

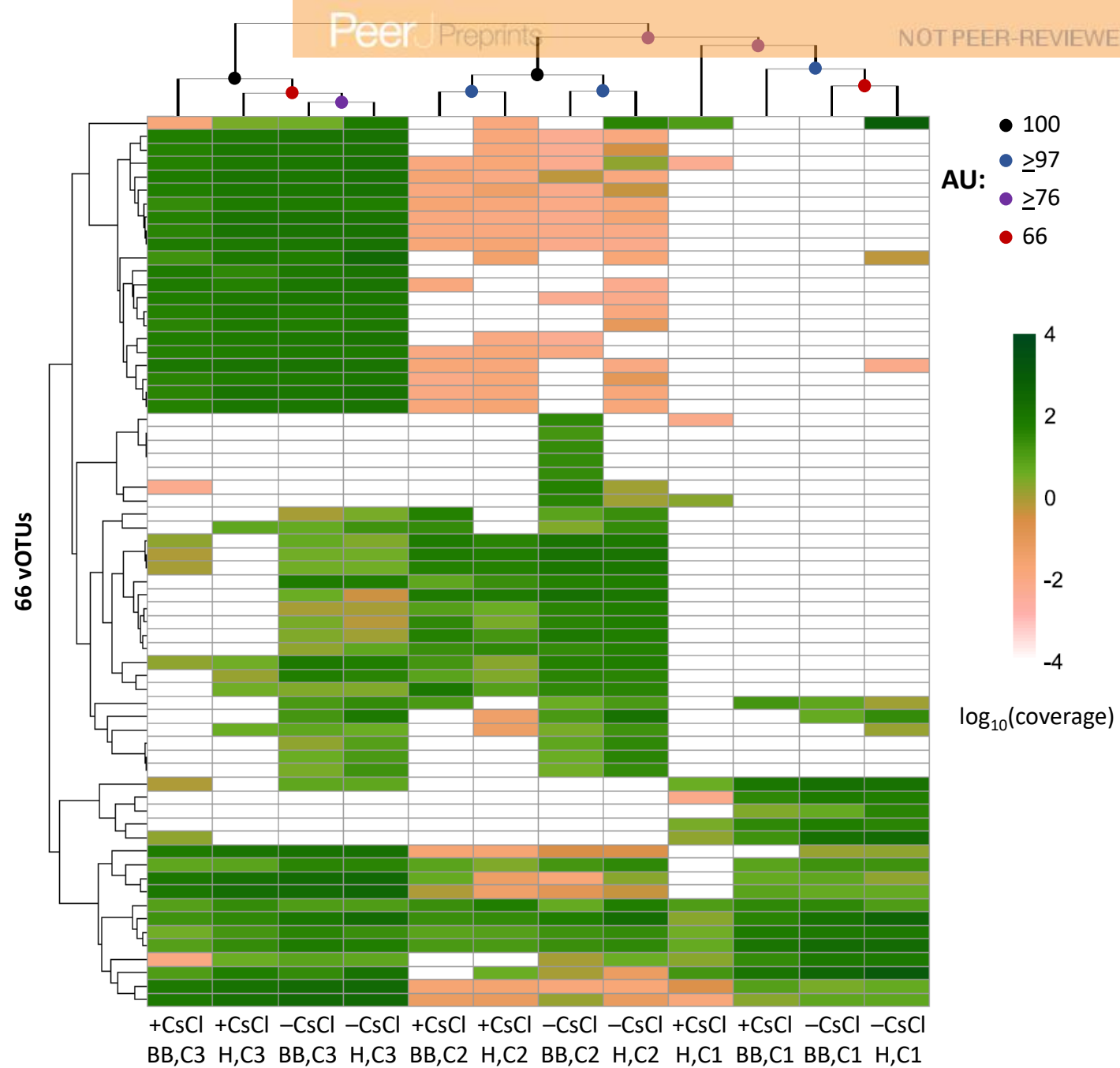


Figure 8(on next page)

Recovery of ssDNA viruses across habitats and methods.

A) ssDNA viral contigs from viromes in Experiment 2. The PowerSoil bog samples are grouped, as are the PowerSoil fen samples. The single Wizard virome from the fen habitat is also shown. B) ssDNA viral contigs from viromes in Experiment 2 grouped by the four treatments: +/- CsCl and bead-beating [BB] or heat [H] virion lysis method. C) ssDNA viruses from both Experiments are shown and grouped by habitat.

